Automated Design of Waveguide Components Using Hybrid Mode-Matching/Numerical EM Building-Blocks in Optimization-Oriented CAD Frameworks—State-of-the-Art and Recent Advances

Fritz Arndt, *Fellow, IEEE*, Ralf Beyer, Jan M. Reiter, Thomas Sieverding, *Member, IEEE*, and Tomas Wolf

(Invited Paper)

***Abstract*— Fast hybrid mode-matching/boundary-contour (MM/BC) and mode-matching/finite-element (MM/FE) waveguide building blocks are described for the optimization-oriented use in powerful circuit computer-aided design (CAD) tools and the automated design of waveguide components. The efficient electromagnetic (EM) CAD technique allows the accurate design of a comprehensive class of rectangular and circular waveguide components including realistic structures of higher complexity. The efficiency and flexibility of the hybrid CAD method is demonstrated at advanced EM design examples, such as broad-band circular-to-rectangular waveguide transitions including octagonal cross sections, waveguide resonator filters with rounded corners, optimum-shaped bends, dual-mode filters with coupling sections without tuning screws, ridged waveguide filters with rounded corners, and multiplexers. The designed components are directly amenable to cost-efficient fabrication techniques like computer-controlled milling methods. The theory is verified by available measurements.**

***Index Terms*— Boundary integral equations, design automation, diplexers, finite-element methods, mode-matching methods, multimode waveguide, waveguide components, waveguide discontinuities, waveguide filters, waveguide transitions.**

I. Introduction

THE ADVANCED design of waveguide components for which accuracy, performance, and development time are critical design parameters requires reliable and fast electromagnetic (EM) computer-aided design (CAD) tools. This allows the direct utilization of modern fabrication techniques, such as computer-controlled milling, die casting, or electroforming methods, without the need for post-assembly tuning elements. The advantages are reduced manufacturing costs and development time, as well as improved performance. Moreover, components without tuning screws show better passive inter-modulation (PIM) features and power handling capacity.

With the steadily growing requirements and increased specifications, and in view of the availability of high-performance low-cost computers, the desirable goal is to go beyond the traditional use of EM simulators for mere validation and analysis purposes. It is to develop and utilize EM building blocks which are fast enough to allow the direct application of matured optimizers and CAD tools, and also for waveguide components of more general shape.

For components composed of rectangular and circular waveguide structures, efficient mode-matching building blocks have already been developed in the past (e.g., [1]–[6]). As has been successfully demonstrated, these allow the rigorous and fast CAD of the large class of waveguide components, which are compatible with the Cartesian or cylindrical coordinate system, such as transformers, filters, multiplexers, couplers, phase shifters, polarizers etc., [1]–[18]. The extremely high interest in direct, slightly modified, or renamed mode-matching techniques for waveguide structures—demonstrated by the large and increasing number of articles devoted to this already well-known subject just recently—may justify some remarks in this paper on the actual state-of-the-art and efficiency of the already available mode-matching building blocks.

For the analysis of more complicated structures, space discretization methods are typically used, such as the three-dimensional (3-D) finite element (FM) [27]–[29] or finite-difference time-domain (FDTD) methods, (e.g., [30], [31]). However, because of the rather high requirements concerning storage capacity and central processing unit (CPU) time for the CAD of such structures, adequate hybrid methods are desirable which combine the advantages of both the flexibility of the space discretization methods with the efficiency of the mode-matching method. A combined mode-matching/finite-element (MM/FE) method has been proposed for the design of dual-mode filters in [32], [33]. In [34], a boundary contour mode-matching (BCMM) method is applied for the full-wave modal analysis of arbitrarily shaped H- and E-plane discontinuities.

Recent advances in the development of efficient circuit theory CAD software have stirred the interest in interfacing rigorous EM simulators into commercial CAD frameworks [21]–[26]. Also in [35], [36], this approach was just started

Manuscript received September 17, 1996; revised January 13, 1997.

The authors are with the Microwave Department, University of Bremen, D-28334 Bremen, Germany.

Publisher Item Identifier S 0018-9480(97)03097-4.

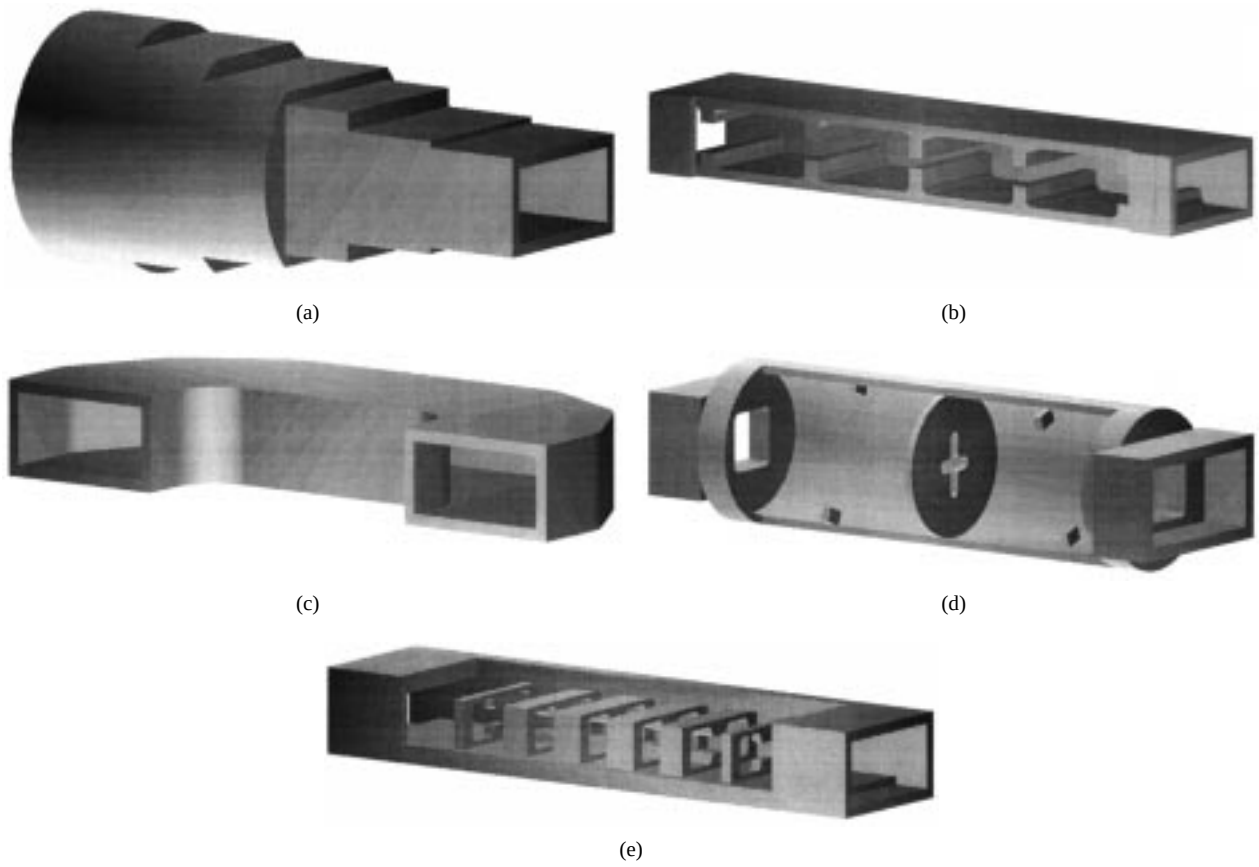

Fig. 1. Design examples for the hybrid EM CAD technique based on fast mixed BCMM and MM/FE waveguide building blocks. (a) Broad-band circular-to-rectangular waveguide transitions including octagonal cross sections. (b) Waveguide resonator filters with rounded corners. (c) Optimum-shaped broad-band bends for feed-network applications. (d) Dual-mode filters with coupling sections without screws. (e) Ridged waveguide filters with rounded corners.

with a circuit model for the simple H-plane rectangular waveguide step problem. This may underline the high actuality of this topic. All necessary basic rectangular and circular waveguide mode-matching building blocks have been implemented in common circuit CAD tools [22]–[26], and the fast and user-friendly CAD of nearly all usual components based on rectangular and circular waveguide structures has been demonstrated in [22]–[24].

In this paper, fast hybrid mode-matching/boundary-contour (MM/BC) and MM/FE waveguide building blocks are described for the optimization-oriented use in powerful circuit CAD tools and the automated design of advanced waveguide components which include structures of more general shape. Design examples are broad-band circular-to-rectangular waveguide transitions including octagonal cross sections [Fig. 1(a)], waveguide resonator filters with rounded corners [Fig. 1(b)], optimum-shaped broad-band bends for feed-network applications [Fig. 1(c)], dual-mode filters with coupling sections without tuning screws [Fig. 1(d)], and ridged waveguide filters with rounded corners [Fig. 1(e)]. The hybrid technique is based on the MM/FE [32] and the BCMM methods [34] which combine wide flexibility with high efficiency. Encouraged by the efficient network optimization capabilities of modern circuit theory CAD tools, a straightforward dual-mode filter design approach is presented which yields excellent starting values for the subsequent fine optimization.

II. Theory

A. Mode-Matching Key Building Blocks for Rectangular and Circular Waveguide Structures

It has been demonstrated that merely four mode-matching key building blocks are the basis for the accurate and fast simulation of the comprehensive class of rectangular and circular waveguide structures—the asymmetric rectangular waveguide double-plane step discontinuity [1], [37], the asymmetric rectangular-to-circular [1], [5], and circular-to-circular waveguide step discontinuities [1], as well as the general six-port cross [4] (which is reducible to T-junctions [2], magic-Tee structures [38], or corners by placing adequate short-circuit planes). The combination of these key building blocks with homogeneous rectangular or circular waveguide sections of finite lengths by the generalized scattering matrix (GSM), generalized admittance matrix (GAM), or generalized impedance matrix (GIM) techniques (cf. [1]–[13]), leads to the usual full-wave mode-matching building blocks,[1] such as rectangular, circular, or multiple irises of finite thickness, cavities of finite lengths, single and multiple metal inserts, T-

[1] Basic mode-matching/numerical EM waveguide elements, like irises, T-junctions, bends, post sections, etc., for building waveguide components via homogeneous waveguide sections of finite length are designated as *building blocks*. They may be derived from mode-matching *key building blocks*, like the T-junction from the six-port cross.

junctions, crosses, etc. A complete set of these mode-matching building blocks is already available in implemented form for the convenient use in common circuit CAD tools [22]–[26].

All efficiency features inherent in the most advanced mode-matching techniques are consequently utilized to allow the extremely fast EM CAD of rectangular and circular waveguide components. These include, in particular, a modified algorithm [1], [9], which requires only the inversion of a submatrix with a quarter of the size of the more conventional mode-matching technique described in the rather classic [37], which is often cited in this context. Moreover, the related submatrix is merely of the order of the lower number of modes in the smaller waveguide section due to an automatic determination process of the appropriate number of modes which are selected conveniently in the order of increasing cutoff frequency [39]. The asymmetric step discontinuities already include the full information required for general multiport transitions or multiaperture irises (cf. [3]). Coupling section elements of finite lengths (e.g., irises or metal inserts) are combined by considering two junctions at once [9], where again, only one submatrix of reduced size has to be inverted (a similar technique has been recently described again [40]).

The coupling integrals are solved analytically (with the exception of the step discontinuity larger circular-to-smaller rectangular which is calculated as a contour integral numerically by a fast Gaussian quadrature method [5]). Furthermore, for two-port structures, the frequency dependency of the coupling integrals can be eliminated as is already well known [1], [3], [9], [37]. If the described efficiency features are utilized, a solid and fair comparison between the possible adequate generalized matrix combination techniques (GSM, GAM, GIM) reveals that, in general, the computational effort for this kind of application is nearly the same for all three techniques. The last two facts are in clear contrast to, for instance, the opinion uttered repeatedly by authors like those of [19], [41], who have recently rediscovered multiple times the eigenfunction solution for standard waveguide step problems (e.g., inductive, capacitive, and double steps) by applying a method of moments modal expansion (e.g., impedance matrix) approach though, by the way, standard textbook knowledge (e.g., [42]) would have been sufficient to verify that the resulting coupling matrices are equivalent to those of the already available and well-documented mode-matching solution if adequately applied to these problems (including the praised frequency independence for the not normalized coupling integrals).[2]

B. Boundary Contour Mode-Matching Method

For arbitrarily shaped discontinuities in the H- or E-plane of rectangular waveguides [such as cavities with rounded corners, Fig. 1(b), or optimized bends, Fig. 1(c)], the very efficient BCMM technique [34] is applied. In contrast to other techniques, such as the boundary integral method adapted very recently to this problem [43], which provide only the fundamental TE_{10} mode information at the port waveguides, the complete *modal* scattering matrix of the corresponding region is obtained, i.e., the necessary higher order mode information for the arbitrary combination of such structures is available *directly*. Moreover, it is not necessary to first search for the eigenfunctions.

For the key-building block discontinuity, Fig. 2(a), the tangential field components of the TE- (index h) and TM-waves (index e) are formulated at the corresponding reference plane(s) i by

$$\vec{E}_t^{(i)} = \sum_{j=1}^{M} \sqrt{Z_j^e}\,\vec{e}_j^{\,e}(a_j^e + b_j^e) + \sqrt{Z_j^h}\,\vec{e}_j^{\,h}(a_j^h + b_j^h) \tag{1}$$

$$\vec{H}_t^{(i)} = \sum_{j=1}^{M} \sqrt{Y_j^h}\,\vec{h}_j^{\,h}(\mp a_j^h \pm b_j^h) + \sqrt{Y_j^e}\,\vec{h}_j^{\,e}(\mp a_j^e \pm b_j^e) \tag{2}$$

where $\vec{n}$ is the normal unity vector, Z and Y are the corresponding wave impedances or admittances, respectively, and $\vec{e}$ and $\vec{h}$ are the normal mode functions which are related to the potential functions ψ in the usual manner. The expressions for the transverse mode vectors $\vec{e}$ and $\vec{h}$ are given in [34].

The boundary condition for the electric field yields the system of linear equations

$$\boldsymbol{T}\vec{\alpha} = \boldsymbol{E}(\vec{a} + \vec{b}) \tag{3}$$

where the elements of the matrix $\boldsymbol{T}$ are the coupling integrals of the field vectors of the cavity region. Due to the nonorthogonality of these field vectors at the boundary, this matrix is not diagonal. The matrix $\boldsymbol{E}$ describes the expansion of the electric field in the waveguide ports by the cylindrical wave functions in the cavity region [34].

The boundary conditions for the magnetic field at the waveguide ports yield the remaining k sets of equations in the form

$$-\vec{a} + \vec{b} = \frac{1}{j\eta}\,\boldsymbol{E}^T\vec{\alpha} \tag{4}$$

where η is the free-space wave impedance and the superscript T denotes the transpose. The excitation coefficients $\vec{\alpha}$ can be eliminated by using (3), which yields

$$(-\vec{a} + \vec{b}) = \boldsymbol{C}(\vec{a} + \vec{b}) \tag{5}$$

with

$$\boldsymbol{C} = \frac{1}{j\eta}\,\boldsymbol{E}^T\boldsymbol{T}^{-1}\boldsymbol{E}. \tag{6}$$

The desired full-wave scattering matrix $\boldsymbol{S}$ of the general k-port waveguide junction is then given by

$$\boldsymbol{S} = (\boldsymbol{I} - \boldsymbol{C})^{-1}(\boldsymbol{I} + \boldsymbol{C}) \tag{7}$$

with the identity matrix $\boldsymbol{I}$.

[2] In fact, the authors of this paper have verified on several computers, CRAY J90, IBM SP2, Pentium PC, that e.g., for an inductive iris filter cited in [41], unlike the opinion of the concerned authors, the impedance matrix approach [41] is about four to five times *slower* than our advanced generalized s-matrix technique described here.

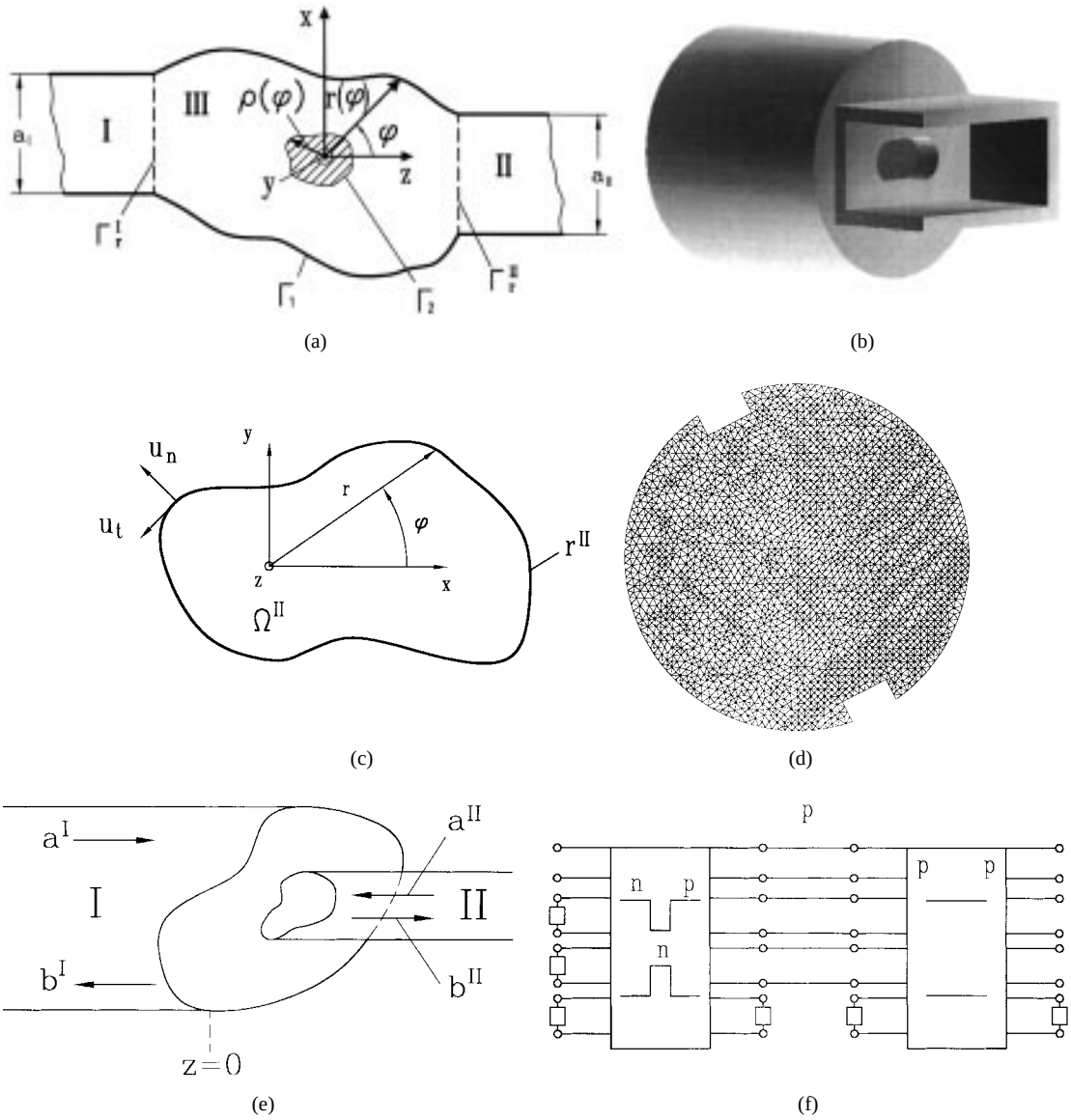

Fig. 2. Arbitrarily shaped waveguide discontinuities. (a) Key-building block discontinuity for the BCMM technique. (b) Arbitrarily shaped iris with finite thickness modeled by the CIMM method. (c) Arbitrarily shaped iris with finite thickness modeled by the CIMM method. (d) Finite-element mesh for the post coupling section in the dual-mode filter of Fig. 1(d). (e) Discontinuity of arbitrarily shaped waveguides. (f) Combination of the building blocks (e.g., arbitrarily shaped iris) with an empty waveguide section by p accessible modes.

C. Contour-Integral Mode-Matching Technique

For the simulation of the arbitrarily shaped iris with finite thickness between two different waveguides, Fig. 2(b), either the hybrid MM/FE method (described in Section II-D) or the contour-integral mode-matching (CIMM) method [45] may be applied. For iris shapes with only moderate variation of the amplitude of contour function $r(\varphi)$ [Fig. 2(b)and 2(c)], the CIMM method is more convenient and yields fast results. For more complicated cross sections, such as coupling structures for dual-mode filters [Fig. 2(d)] where a high number of higher order modes may be involved, the ME/FE method is faster.

In the cross section with the analytically or numerically given contour function $r(\varphi)$ of the arbitrarily shaped iris, the fields are expanded in terms of the complete set of cylindrical wave functions

$$T(r,\,\varphi) = \sum_{n=0}^{N} J_n(k_c r)[a_n\,\cos(n\varphi) + b_n\,\sin(n\varphi)]. \quad (8)$$

The set is then multiplied with appropriate weighting functions $\cos(j\varphi)$, $\sin(j\varphi)$, and integrated along the contour in order to satisfy the given field periodicity with respect to the angular coordinate φ. This relates the still unknown coefficients a_n, b_n in (8) and the Fourier coefficients α_j, β_j resulting from the contour integration, in the following manner:

$$\alpha_j = \sum_{n=0}^{N} \left[\int_0^{2\pi} J_n(k_c r) a_n\,\cos(n\varphi)\,\cos(j\varphi)\,d\varphi + \int_0^{2\pi} J_n(k_c r) b_n\,\sin(n\varphi)\,\cos(j\varphi)\,d\varphi \right] \quad (9)$$

$$\beta_j = \sum_{n=0}^{N} \left[\int_0^{2\pi} J_n(k_c r) a_n \cos(n\varphi) \sin(j\varphi)\, d\varphi + \int_0^{2\pi} J_n(k_c r) b_n \sin(n\varphi) \sin(j\varphi)\, d\varphi \right]. \quad (10)$$

The requirement that the tangential electric-field strength along the iris boundary contour is zero yields a homogeneous system of equations which may be written in matrix form

$$\begin{pmatrix} \alpha \\ \beta \end{pmatrix} = \underbrace{\begin{bmatrix} [CC] & [SC] \\ [CS] & [SS] \end{bmatrix}}_{[C]} \underbrace{\begin{pmatrix} a \\ b \end{pmatrix}}_{x} = 0 \quad (11)$$

where the submatrices are denoted according to the sin- and cos-terms in (9) and (10). The nontrivial solutions of this system of (11) result from $\det[C] = 0$ which yields the eigenvalues, i.e., the cutoff wavenumbers k_c, of the iris waveguide section of arbitrary shape and finite length. The eigenvalues and the eigenvectors a, b are calculated by the singular value decomposition (SVD) method [46].

The modal scattering matrix of the discontinuity at $z = 0$ is obtained in the usual form, by matching of the tangential field components. Application of the orthogonality of the eigenfunctions and rearranging the equations yields the modal scattering matrix of the discontinuity directly. For simplification, all double integrals are reduced to contour integrals.

D. Hybrid MM/FE Method

For structures which require a high number of eigenmodes to be considered and which may include sharp edges, like the coupling elements of the dual-mode filter in Figs. 1(d) and 2(c), the hybrid MM/FE method [32], [33] is applied because of its high efficiency. In contrast to other methods, like the boundary integral equation approach [44] recently reported, no search procedure for the detection of eigenvalues is necessary where the resulting computation time can be rather long, especially if optimization routines are used. All desired eigenvalues are calculated immediately by an efficient tridiagonal matrix eigenvalue procedure.

The transverse electric $\vec{E}_t$ and magnetic fields $\vec{H}_t$ in each homogeneous waveguide section are represented by scalar potentials [32] which are solutions of the transverse homogeneous Helmholtz equation, satisfy Dirichlet and Neumann boundary conditions on perfectly conducting electric and magnetic walls, and show the usual orthonormal properties.

The initial mesh for the two-dimensional (2-D) finite-element method (FEM) solution of the Helmholtz equation for the sections with nearly arbitrary geometry is generated by the Delaunay triangulation; the mesh can locally be refined and optionally be smoothed [28], [47], [48]. The generalized matrix eigenvalue problem is reduced to tridiagonal form by the Lanczos procedure [47], with application of a shift and invert technique to accelerate convergence. Full Gram–Schmidt type re-orthogonalization guarantees the orthogonality of even higher order multiple degenerate modes. The system of equations arising in each Lanczos iteration step is solved by sparse matrix Cholesky decomposition using the minimum degree algorithm [49].

Matching the transverse EM fields $\vec{E}_t$ and $\vec{H}_t$ at the common interface of a general waveguide step discontinuity [Fig. 2(e)] leads to the set of matrix equations for the amplitude vectors $a_{\mathrm{I,\,II}}$ and $b_{\mathrm{I,\,II}}$ of the incident and scattered waves in waveguide I and II, respectively [32]. From this set of equations, the GSM of the complete step discontinuity is obtained.

E. Generalized Scattering Matrix Combination

For the investigated class of waveguide components, the combination of the waveguide building blocks is provided by the GSM technique [1], [2], [4]–[12]. For the corresponding intermediate homogeneous rectangular or circular waveguide section of length l (for instance, the cavity length between two irises), the modal scattering matrix is given by

$$\boldsymbol{S}_{wg} = \begin{bmatrix} \boldsymbol{O} & \boldsymbol{D} \\ \boldsymbol{D} & \boldsymbol{O} \end{bmatrix}, \qquad \boldsymbol{D} = \mathrm{diag}\{e^{-\gamma_p l}\}. \quad (12)$$

This leads to a straightforward multimode equivalent circuit description [Fig. 2(f)] where the cascaded building blocks are connected by modal transmission lines (i.e., for each mode by one transmission line). This allows the convenient implementation in common circuit CAD tools [23]–[26].

It has turned out that for typical microwave components (e.g., a filter), only a few higher order modes have to be taken into account in the homogeneous waveguide (cavity) section. For instance, two higher order modes (i.e., a total number of $p = 3$ modes) already give reliable results [24] even for filters where the next propagating mode, e.g., TE_{20}, is utilized for obtaining stopband poles, a technique which has been already proposed seven years ago [50] (and has been rediscovered just recently [51]). Moreover, the example of the high-power elliptic function $\mathrm{TE}_{103}/\mathrm{TE}_{201}$-mode filter in [24] demonstrates that by suitable optimization—in contrast to the opinion in [51]—the transmission zeros can be placed very close to the passband of the filter in order to obtain an extremely high edge steepness.

Although the authors investigated the (modal) GAM or generalized impedance matrix (GIM) for the building blocks for comparison purposes as well (e.g., [3]), the GSM technique was preferred. As has already been mentioned, it has turned out (if all features of the most advanced mode-matching techniques (cf. Section II-A) are utilized) that, in general, the computational effort for this kind of application is nearly the same for all three techniques. This is particularly true if, like in many cases, a very different number of localized and accessible modes has advantageously been chosen for the building blocks and for the combining waveguide section, respectively. As is well-known, this requires inversions of Y- or Z-submatrices of high order for the calculation of the S-matrix (e.g., [13]). For the GSM technique, at the S-matrix of the step discontinuity of an iris

$$\begin{aligned} \boldsymbol{S}_{11} &= -\boldsymbol{E} + \boldsymbol{V}\boldsymbol{S}_{21} \\ \boldsymbol{S}_{12} &= \boldsymbol{V}[\boldsymbol{E} + \boldsymbol{S}_{22}] \\ \boldsymbol{S}_{21} &= 2\boldsymbol{T}^{-1}\boldsymbol{V}^t \\ \boldsymbol{S}_{22} &= \boldsymbol{T}^{-1}[\boldsymbol{E} - \boldsymbol{V}^t\boldsymbol{V}] \end{aligned} \quad (13)$$

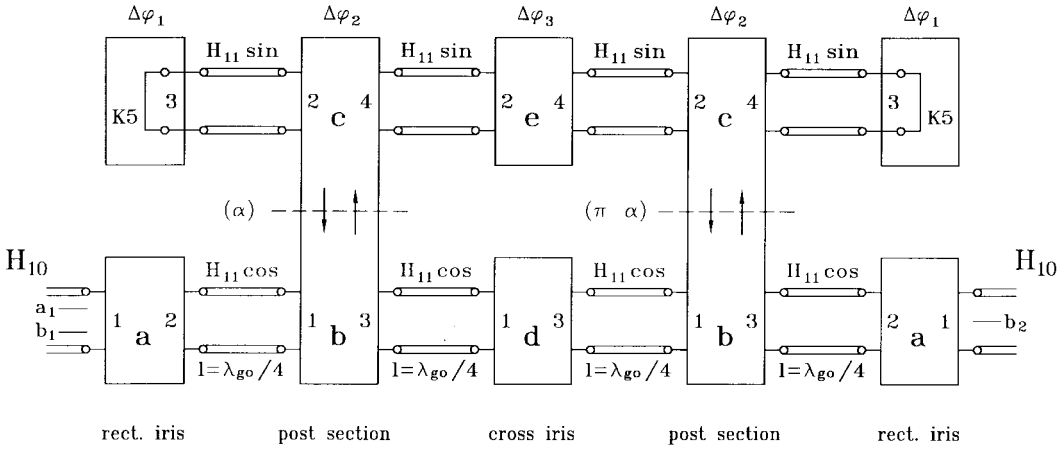

Fig. 3. Equivalent circuit for the efficient CAD of a four-pole dual-mode filter [cf. Fig. 1(d)].

only a submatrix of order n, n (with n being the low number of modes in the smaller waveguide) $\boldsymbol{T} = \boldsymbol{E} + \boldsymbol{V}^t\boldsymbol{V}$ has to be inverted. The coupling matrix $\boldsymbol{V}$ is given for rectangular and circular waveguide discontinuities analytically [1], and it contains frequency independent terms which are only determined by the geometry.

F. Direct EM Cohn Synthesis of Single-Mode Filters

The most prudent approach for the fast and accurate Chebychev filter design is the combination of the conventional Cohn filter synthesis [52] with EM simulation subroutines for the conversion of the impedance inverter data K, ϕ into geometrical parameters [18], [53]. The corresponding general relations between the complex scattering parameter $\boldsymbol{S}_{11}$ obtained by the mode-matching subroutine and the parameters K and ϕ are given in [55].

G. Design of Dual-Mode Filters

Dual-mode filters [60] are particularly attractive for satellite communications applications. A large overview of possible synthesis and design methods is available in [18]. More recently, a design based on the low-pass prototype procedure of [61] has been presented in [17].

Encouraged by the efficient network optimization capabilities of modern circuit theory CAD tools, the authors of the present paper propose a straightforward approach which utilizes the direct optimization of an adequate equivalent circuit (cf. Fig. 3 for a four-pole filter). This allows the fast and immediate CAD of dual-mode filters without an analytic network prototype synthesis calculation.

The chosen equivalent circuit parameters in Fig. 3 related to a real dual-mode filter structure [for instance, Fig. 1(d)] are: a transmission first (last) iris; $\Delta\varphi_1$ reflection phase difference H_{11}^c/H_{11}^s caused at first (last) iris; b reflection parameter at the coupling post structure for H_{11}^c; c reflection parameter at the coupling post structure for H_{11}^s; $\Delta\varphi_2$ phase difference H_{11}^c/H_{11}^s caused at the coupling post structure; α physical angle of rotation of the coupling post structure (for fine adjusting of the coupling between H_{11}^c/H_{11}^s); d transmission of cross iris for H_{11}^c; e transmission of cross iris for H_{11}^s; $\Delta\varphi_3$ phase difference H_{11}^c/H_{11}^s caused at the cross iris; λ_{g0} guide wavelength at midband frequency.

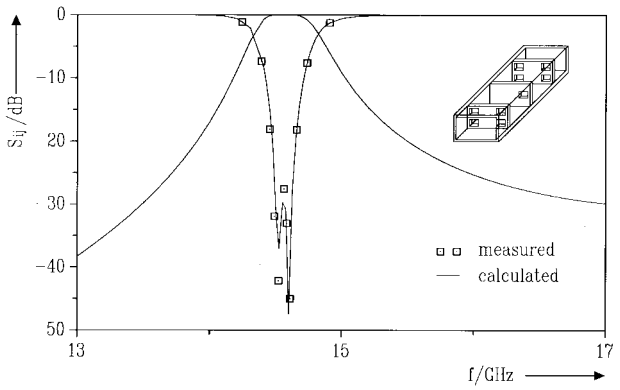

Fig. 4. Optimized multiaperture coupled iris filter. Verification with measurements [3]. WR-62 waveguide. Iris and resonator dimensions in mm: waveguide 15.799 × 7.899; iris thickness 0.21; resonator length 12.155; irises 5.0 × 3.0; displacements of the first and third irises 2.47, 0.5 from the waveguide side walls, or top and bottom walls, respectively; displacement of the middle iris 2.133 from the sidewall; the filter is symmetric in length dimension.

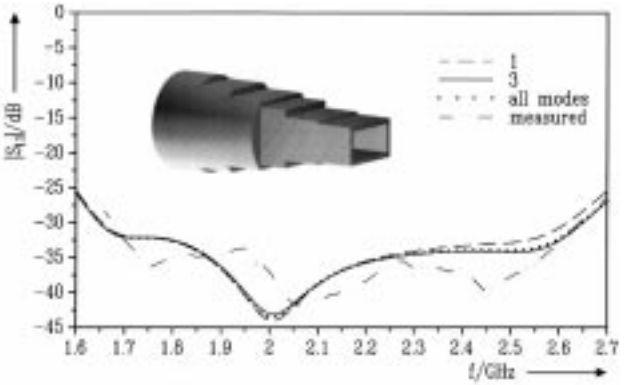

Fig. 5. Broad-band transition from circular-to-rectangular waveguide including octagonal cross sections with rounded corners, compared with available measurements [62]. Dimensions cf. [62].

The steps for the design are as follows.

Step 1) Pre-optimization of the chosen (frequency independent) equivalent circuit parameters for a given

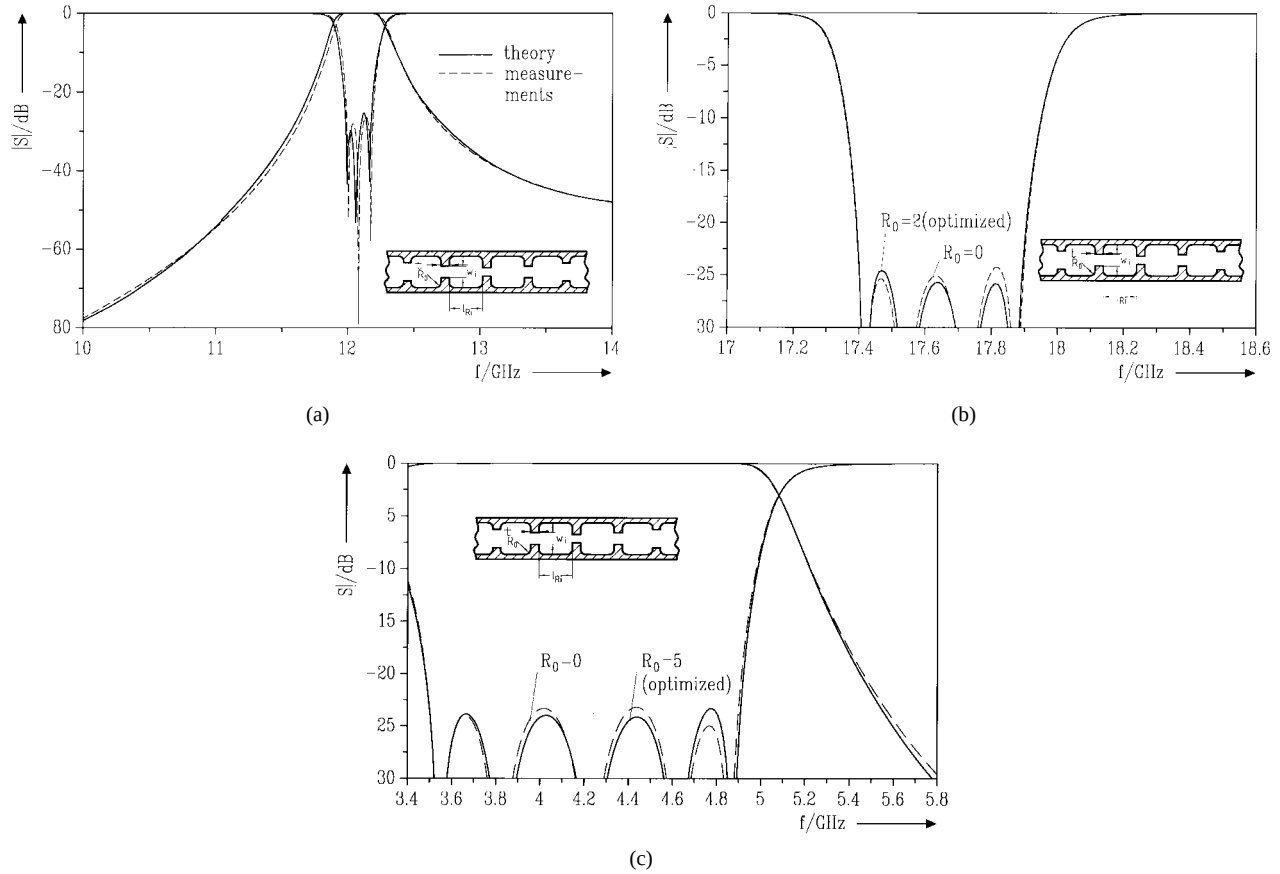

Fig. 6. H- and E-plane iris filters with rounded corners. (a) Comparison between theory and measurements at a three-cavity H-plane filter example of [43], WR-75 waveguide. (b) Influence of the finite radius on a typical four-resonator H-plane filter for wireless communications applications, WR-51 waveguide, original dimensions (mm): $a = 12.954$, $t = 3.5$, $w_1 = 7.720$, $w_2 = 5.757$, $w_3 = 5.413$, $l_{R1} = 7.846$, $l_{R2} = 9.260$, $R_0 = 2$, dimensions after the re-optimization: $1.0025w_1$, $1.0015w_2$, $1.0010w_3$, $1.0035l_{R1,2}$. (c) Influence of the finite radius on a typical E-plane C-band filter, dimensions (mm): $a = 46$, $b = 29.083$, $w_1 = 17.701$, $w_2 = 11.0850$, $w_3 = 8.160$, $t = 3$, $l_{R1} = 20.432$, $l_{R2} = 17.244$, $_{R3} = 15,820$, $R_0 = 2$, dimension after the re-optimization: $1.0200w_1$, $0.9855w_2$, $0.9550w_3$, $1.0278l_{R1,2,3}$.

specification for the filter where the rectangular iris $\boldsymbol{S}_{\text{iris}}$, the post structure $\boldsymbol{S}_{\text{post}}$, and the cross iris $\boldsymbol{S}_{\text{cross}}$ are modeled by the equivalent circuit parameters for the fundamental modes H_{10}, H_{11}^c, H_{11}^s as follows:

$$\boldsymbol{S}_{\text{iris}} = \begin{bmatrix} -\sqrt{1-a^2} & -ja & 0 \\ -ja & -\sqrt{1-a^2} & 0 \\ 0 & 0 & -\exp(j\Delta\varphi_1) \end{bmatrix} \tag{14}$$

$$\boldsymbol{S}_{\text{post}} = \begin{bmatrix} \boldsymbol{S}_{11} & \boldsymbol{S}_{21} & \boldsymbol{S}_{31} & \boldsymbol{S}_{41} \\ \boldsymbol{S}_{21} & \boldsymbol{S}_{22} & \boldsymbol{S}_{41} & \boldsymbol{S}_{42} \\ \boldsymbol{S}_{31} & \boldsymbol{S}_{41} & \boldsymbol{S}_{11} & \boldsymbol{S}_{21} \\ \boldsymbol{S}_{41} & \boldsymbol{S}_{42} & \boldsymbol{S}_{21} & \boldsymbol{S}_{22} \end{bmatrix} \tag{15}$$

where[3]

$$\begin{aligned} \boldsymbol{S}_{11} &= -jb\cos^2\alpha - jc\exp(j\Delta\varphi_2)\sin^2\alpha \\ \boldsymbol{S}_{21} &= jb - jc\exp(j\Delta\varphi_2)\sin\alpha\cos\alpha \\ \boldsymbol{S}_{31} &= \sqrt{1-b^2}\cos^2\alpha + \sqrt{1-c^2} \\ &\quad \cdot \exp(j\Delta\varphi_2)\sin_2\alpha \\ \boldsymbol{S}_{41} &= [-\sqrt{1-b^2} + \sqrt{1-c^2}\exp(j\Delta\varphi_2)] \\ &\quad \cdot \sin\alpha\cos\alpha, \\ \boldsymbol{S}_{22} &= -jb\sin^2\alpha - jc\exp(j\Delta\varphi_2)\cos^2\alpha \\ \boldsymbol{S}_{42} &= \sqrt{1-b^2}\sin^2\alpha + \sqrt{1-c^2} \\ &\quad \cdot \exp(j\Delta\varphi_2)\cos^2\alpha \end{aligned}$$

as in (16), shown at the bottom of the next page.

Step 2) Calculation of the cross iris geometries according to the parameters d, e; adjustment of $\Delta\varphi_3$ and adjustment of $\Delta\varphi_1$, $\Delta\varphi_2$.

Step 3) Calculation of the cutoff frequency of the post structure for the given $\Delta\varphi_2$; readjustment of the structure geometry according to b, c; selection of the length of the structure according to $\Delta\varphi_2$; adjustment of the rotation angle α.

Step 4) Calculation of iris 1, 2 for the given a, adjustment of $\Delta\varphi_1$ by changing the iris height.

Step 5) Calculation of the resonator lengths.

Step 6) Rigorous analysis of all irises and the post structure with the MM/FE method.

Step 7) Adjustment of the resonator lengths, lengths of post structure, and angle α according to the rigorous scattering parameters.

[3]For the second post structure, the signs of $\boldsymbol{S}_{11}$, $\boldsymbol{S}_{41}$ have to be interchanged as the post structure is rotated by $\pi - \alpha$

Step 8) Rigorous GSM analysis of the filter. Readjustment of the resonator lengths.

Step 9) Fine optimization by using the rigorous GSM technique, if required.

H. Automated Design with the Mode-Matching/Numerical EM Building Blocks

All necessary rectangular and circular waveguide mode-matching building blocks (such as the usual iris types, multiple-step discontinuities, multiple septa, E- and H-plane T-junctions, corners, crosses, cavities, circular-to-rectangular waveguide transitions, etc.) have been implemented for the convenient use in common circuit CAD tools [22]–[26]. The building blocks can be modeled with up to about 300 modes (or more, depending on the available storage resources). Due to the circuit theory parameters of these CAD tools, the combination between the building blocks is carried out by modal transmission lines (Fig. 2) where each transmission line stands for one combination mode. Usually, only a few modes are required. In this way, full benefit can be taken of the available schematics input, design, optimization, and graphical user interface capabilities of the familiar CAD tool.

The direct EM Cohn synthesis algorithm has been implemented in a very efficient stand alone computer code for the fast automated EM synthesis of a wide class of waveguide filters [54], such as inductive iris, metal insert, capacitive iris, aperture coupled, and stub loaded filters, including cavities with rounded corners. The rigorous GSM technique is used within this CAD program. The synthesis provides excellent starting values for the included subsequent fine optimization by the proven evolution strategy method [54]–[58]. Since all efficiency features of the mode-matching technique are fully utilized, the synthesis of, e.g., a usual five-resonator inductive iris filter, takes only about 10 s on a Pentium PC.

The described hybrid mode-matching/numerical EM building blocks are implemented in a flexible Fortran computer code for the fast automated CAD of nearly all waveguide components including multiport structures. The CAD is based on a kind of a three-step modified space-mapping approach [59] as follows:

Step 1) Pre-optimization of adequate (frequency independent) equivalent circuit parameters for a given specification (cf. Section II-D for the dual-mode filter example) by using a random optimizer.

Step 2) Optimization via the rigorous EM theory with a gradient optimizer by using merely a coarse model with few modes.

Step 3) Fine optimization via the rigorous EM theory with a high number of modes.

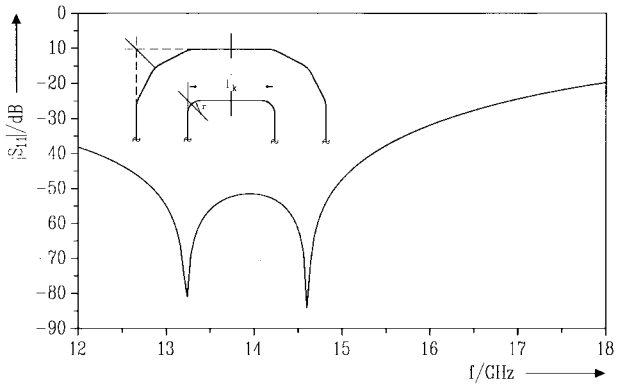

Fig. 7. Broad-band rectangular waveguide bend structure for meander waveguide feed network applications [63], optimized with the BCMM method, WR-62 waveguide $a = 15.798$, $b = 7.899$, $l_k = 5.466$, $r = 0.4$.

III. Results

For the experimental verification of a rectangular waveguide filter, the multiaperture coupled iris filter of [3] has been chosen (see Fig. 4). This filter achieves identical iris shape (for example, suitable for stamping tools), low insertion loss, and high break-down voltage. The filter housing is silver plated, and the 0.21-mm-thick irises are fabricated by etching techniques. Excellent agreement between theory with measurements may be stated. The measured insertion loss is 0.05 dB. The irises have been modeled by inclusion of 100 modes, and only the fundamental mode is necessary to be considered in the cavity region.

In Fig. 5, a broad-band transition from circular-to-rectangular waveguide including octagonal cross sections with rounded corners is compared with available measurements [62]. Here also, the fundamental mode between the discontinuities is sufficient. The step discontinuities including the octagonal structure have been modeled with the MM/FE method by taking all modes into account up to the cutoff frequency of 30 GHz.

The accurate design of rectangular waveguide cavity filters with rounded corners in the H- or E-plane [34] is of high practical interest as increasingly computer-controlled milling, electro-forming, or die-casting techniques are applied for the low-cost fabrication of such filters. Fig. 6(a) shows the comparison between theory and measurements at a three-cavity H-plane filter example of [43]. The iris sections have been modeled by the BCMM method with all modes up to 160-GHz cutoff frequency and only two modes in the cavity regions. The high efficiency of this method is demonstrated by the total CPU time of merely a few seconds for 200 frequency points, on an IBM360 workstation (27 MFlops).

$$\boldsymbol{S}_{\text{cross}} = \begin{bmatrix} -\sqrt{1-d^2} & 0 & -jd & 0 \\ 0 & -\sqrt{1-e^2}\exp(j\Delta\varphi_3) & 0 & -je\exp(j\Delta\varphi_3) \\ -jd & 0 & -\sqrt{1-d^2} & 0 \\ 0 & -je\exp(j\Delta\varphi_3) & 0 & -\sqrt{1-e^2} \end{bmatrix}. \tag{16}$$

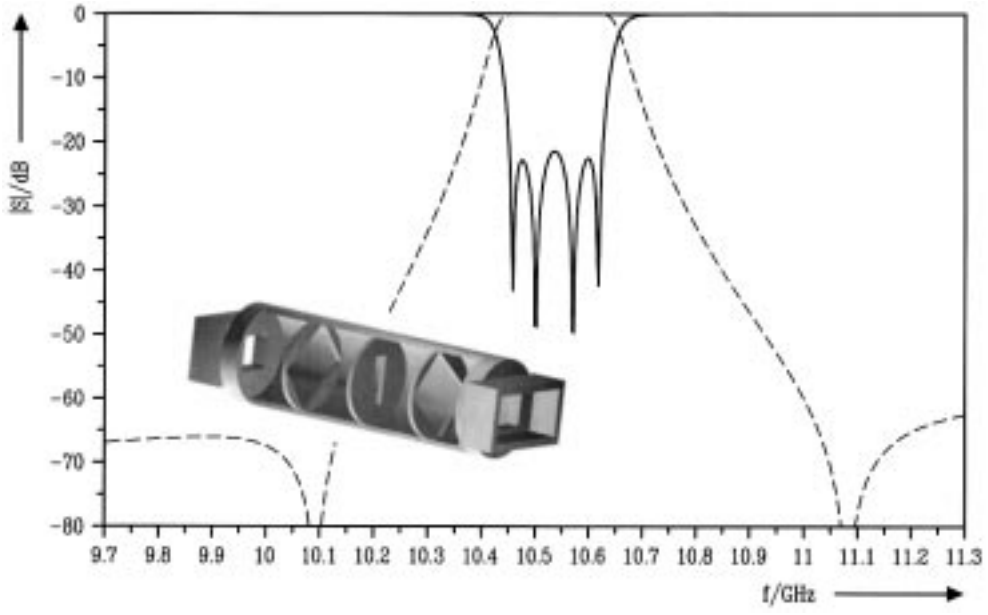

(a)

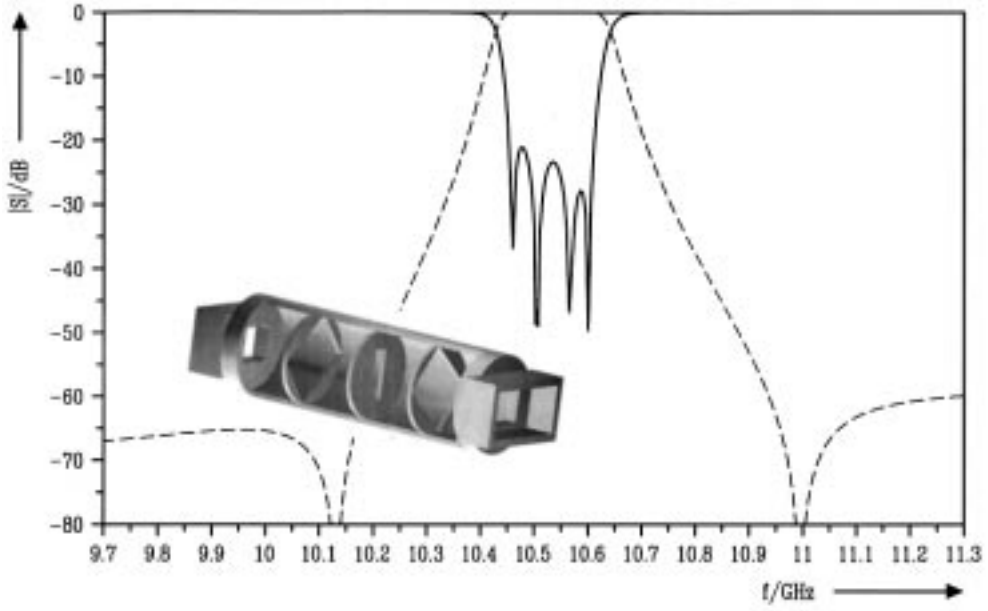

(b)

Fig. 8. Dual-mode filter with rotated iris coupling sections. (a) Results for a filter optimized with the equivalent circuit of Fig. 3, dimensions (mm): WR-90 waveguide, cavity $r = 13$, $l_1 = l_4 = 26.125$, $l_2 = l_3 = 26.443$, irises 11.50 × 10.16, 17.60 × 19.00, 2.70 × 10.00, $t = 1$, $\Delta\varphi_2 = 52.59°$, $\Delta\varphi_4 = 127.41°$. (b) Filter like (a), but with rounded iris corners (radius 0.75 mm), resonator lengths re-optimized $l_1 = l_4 = 27.478$, $l_2 = l_3 = 25.207$.

Fig. 6(b) indirectly demonstrates the influence of the finite radius on a typical five-resonator H-plane filter for wireless communications applications: the desired 24-dB return loss is obtained only by a subsequent second optimization.[4] Fig. 6(c) shows that similar considerations hold for E-plane iris filters. The filters have been pre-synthesized by the direct EM Cohn synthesis (cf. Section II-F) and subsequently optimized by a gradient method.

The efficiency and flexibility of the powerful BCMM method introduced in [34] may be demonstrated furthermore at the successful optimization of broad-band rectangular waveguide bend structures of Fig. 7, which are of high practical importance (e.g., for meander waveguide feed networks for radar slot antennas [63]). As a large number of bends are cascaded there [63], the individual bend has to meet very high return-loss requirements. For this example, all higher order modes up to a cutoff frequency of 380 GHz are included within the complete double-bend structure. For the overall meander structure test, the fundamental mode was sufficient in the interim waveguide sections.

Circular-cavity dual-mode filters have been proposed in the recent past [32], [33], [64]–[65] where the traditional coupling

[4] In Fig. 6(b) and 6(c), only the reoptimized results are shown. The original frequency shift by the not yet optimized values can be verified in [34].

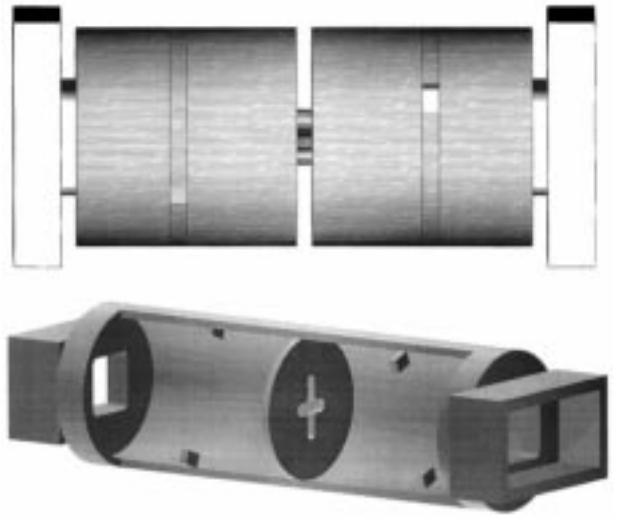

(a)

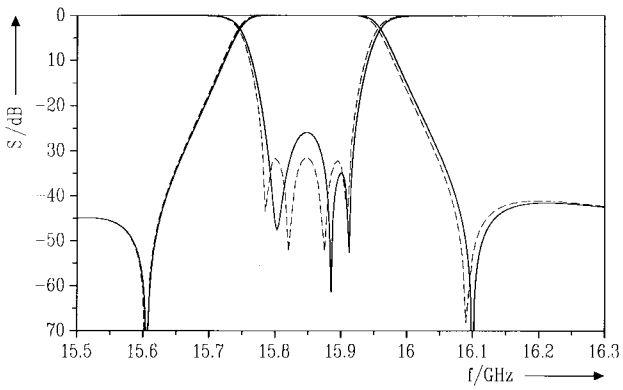

(b)

Fig. 9. (a) Dual-mode filter with a modified post coupling structure. (b) Results for a filter optimized with the equivalent circuit of Fig. 3, dimensions (mm): WR-62 waveguide, cavity $r = 7$, $l_1 = l_4 = 5.968$, $l_2 = l_3 = 7.056$, irises 6.77 × 6.77, $r = 0.5$, $t = 1$, rotated post section 2 × 0.9 × 1.090, $\Delta\varphi = 28.056^\circ$ (first section), 151.944° (second section), cross iris inner width 1.00, radii 0.5, width 3.57, height 6.27, thickness $t = 1.0$.

screws are replaced by structures which may be more convenient for modern fabrication techniques. Fig. 8(a) demonstrates the optimized results with the method described above (Fig. 3) for a rotated rectangular iris version [65]. In order to yield better stability concerning coupling section tolerances, $3\lambda_g/2$-resonators are chosen instead of the usual $\lambda_g/2$ design. The discontinuities have been modeled by inclusion of all modes up to a cutoff frequency of 150 GHz (all symmetries utilized), the homogeneous iris sections with 75 GHz. The results for the fundamental H_{11}^c, H_{11}^s mode combination in the cavities (solid line for the return loss) are in such close agreement with the overall full-wave combination that the results have not been plotted. Fig. 8(b) shows the similar structure but with realistic finite radii in the rectangular iris coupling sections (for fabrication purposes). The resonator lengths have been re-optimized in order to meet the same midband frequency.

A modified post-coupling structure [32], [33], [64] is proposed in Fig. 9. The rotation angle of the twin post structure is an additional optimization parameter. Fig. 9(b) shows the

(a)

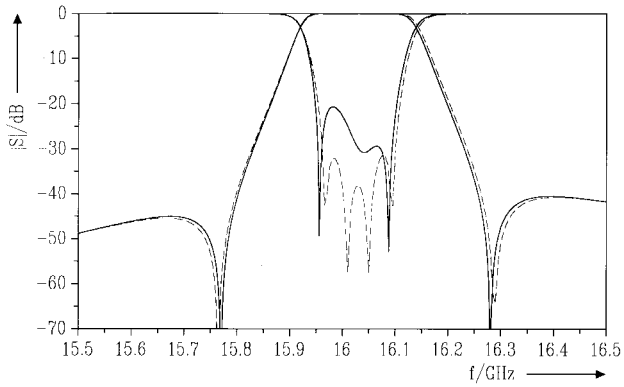

(b)

Fig. 10. (a) Dual-mode filter with inclined elliptical waveguide coupling sections. (b) Results for a filter optimized with the equivalent circuit of Fig. 3, dimensions (mm): WR-62 waveguide, cavity $r = 7$, $l_1 = l_4 = 3.764$, $l_2 = l_3 = 5.803$, irises 6.77 × 6.77, $r = 0.5$, $t = 1$, rotated elliptic waveguide section 7 × 6.75 × 4.3, $\Delta\varphi = 27.7^\circ$ (first section), 152.3° (second section), cross iris inner width 1.00, radii 0.5, width 3.57, height 6.27, thickness $t = 1.0$.

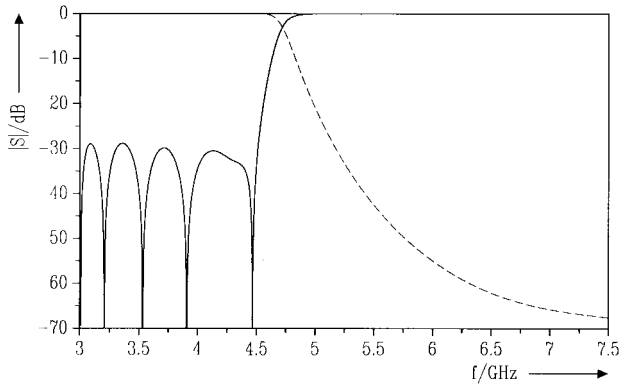

Fig. 11. Ridged waveguide five-cavity low-pass filter with rounded corners. WR-229 in-output waveguide, radii 1.5 mm, overall length 160.9 mm, gap width in all sections 6.7 mm.

results of the equivalent circuit (Fig. 3) optimization (dashed line) and of the subsequent full-wave MM/FE full-wave analysis (solid line). For the full-wave analysis, all modes up to 200-GHz cutoff frequency have been taken into account for the rectangular-to-circular waveguide discontinuities, and 100 GHz for the homogeneous iris and post sections, as well as in the ($\lambda_g/2$-) resonator sections. For the coarse optimization,

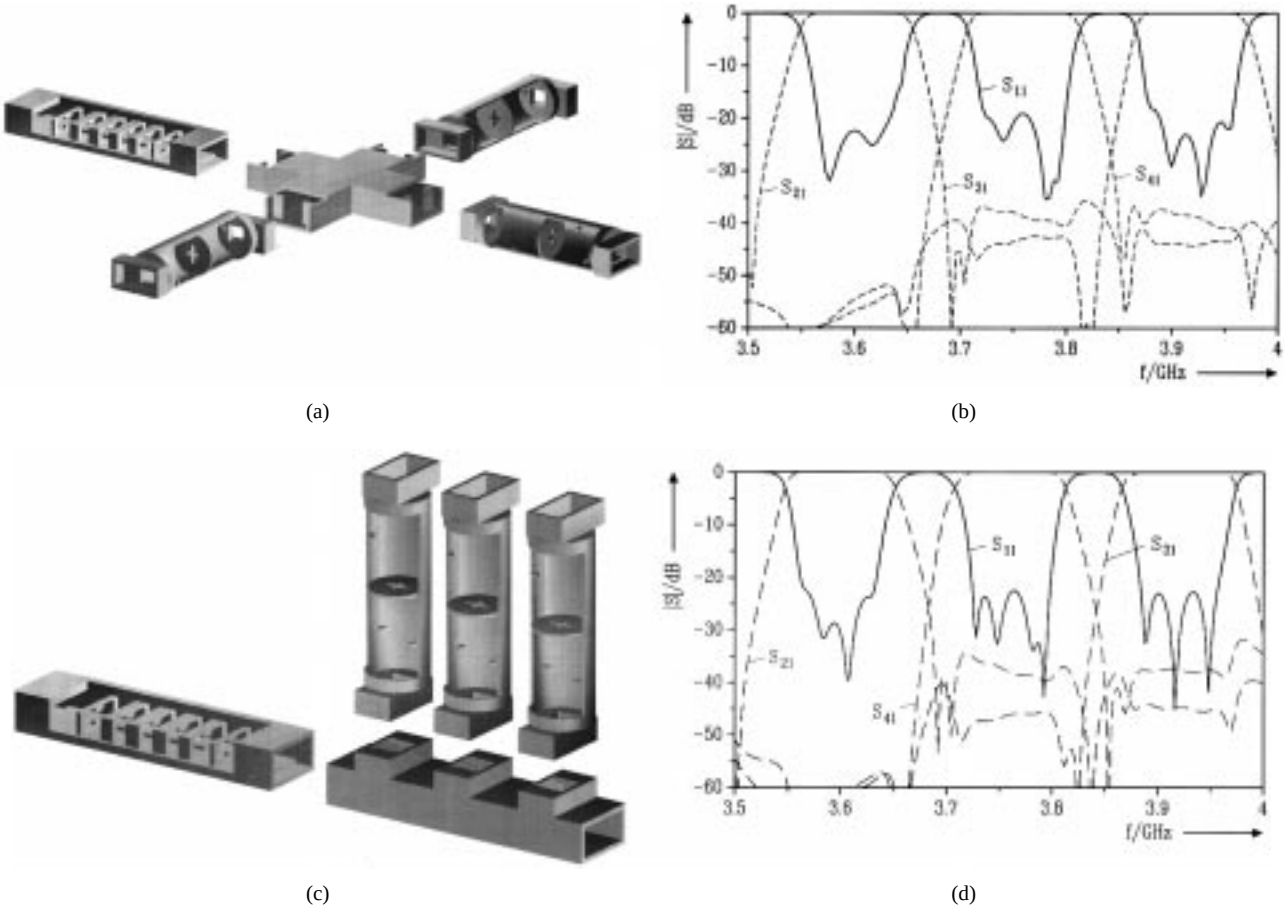

Fig. 12. Complete dual-mode filter OMUX examples including the ridged waveguide PIM filter (Fig. 11). (a) Design with an H-plane cross, dimensions (mm): WR-229 waveguide cross, port 1: no iris, distance cross-plane to ridged waveguide filter plane $l_1 = 33.3$, port 2: distance cross-plane to iris $l_{21} = 24.84$, iris-to-filter plane $l_{22} = 21.57$, iris width $w_2 = 41.25$, port 3: $l_{31} = 35.01$, $l_{32} = 53.02$, $w_3 = 46.83$, port 4: $l_{41} = 36.54$, $l_{42} = 46.17$, $w_4 = 44.68$. Filters: Port 2: cavity $r = 35$, length-to-post section $l_1 = l_4 = 11.206$, length-to-middle iris $l_2 = l_3 = 35.397$, irises with rounded corners ($R = 1.5$, $t = 1$) 1, 3: 28.30 × 27.70; 2: 10.20 × 22.40, post section 15 ×5× 6.933, $\Delta\varphi_1 = 38.537°$, $\Delta\varphi_2 = 141.463°$. Port 3: $r = 35$, $l_1 = l_4 = 7.602$, $l_2 = l_3 = 34.368$, ($R = 1.5$, $t = 1$) 1, 3: 27.0 × 24.0; 2: 9.0 × 21.2, 15 × 5 × 7.955, $\Delta\varphi_1 = 48.075°$, $\Delta\varphi_2 = 133.925°$. Port 4: $r = 13$, $l_1 = l_4 = 8.145$, $l_2 = l_3 = 32.506$; ($R = 1.4$, $t = 1$) 1, 3: 25.8 × 22.5, 2: 9.15 × 20.08; 15 × 5 × 5.891, $\Delta\varphi_1 = 47.232°$, $\Delta\varphi_2 = 132.768°$. (b) Overall analysis of the complete optimized OMUX component with the H-plane cross. (c) Design with a WR-229 waveguide manifold. (d) Overall analysis of the complete optimized OMUX component with the WR-229 waveguide manifold.

merely the fundamental H_{11}^c, H_{11}^s modes are considered in the resonator sections.

In principle, every adequately rotated structure with φ dependence is more or less appropriate for coupling the orthogonal modes in dual-mode filters of the type of Fig. 1(d). For instance, a dual-mode filter with rotated elliptical waveguide coupling sections is shown in Fig. 10(a). Also for this filter type, good starting values (dashed lines) are obtained by the equivalent circuit (Fig. 3) coarse optimization which is illustrated by the subsequent full-wave MM/FE full-wave analysis results (solid line). The number of modes corresponds to those in Fig. 9.

For output multiplexer (OMUX) designs, PIM filters are often required. Fig. 11 show a ridged waveguide low-pass filter design which yields appropriate rejection also for higher order modes (comprising the corresponding TE_{m0} modes ($m > 1$) which are not suppressed, for example, by standard E-plane corrugated filters). Rounded corners are included in the design in order to allow easy computer-controlled milling fabrication and to enable high-power applications. Therefore, also the gap width in the ridge sections is chosen to be appropriately large. At the discontinuities, all modes up to 100-GHz cutoff frequency are included; in the resonator and transformer sections, only seven modes have turned out to be sufficient for accurate modeling.

The high flexibility and efficiency of the proposed hybrid mode-matching/numerical EM CAD method may be demonstrated at the design of complete dual-mode filter OMUX examples (Fig. 12) without additional tuning screws, including the ridged waveguide PIM filter (Fig. 11). The complete optimization is carried out with commercial CAD tools where the T-junctions, crosses, and compensation irises are implemented as modal building blocks, and the modal S-parameters of the already optimized filters are included as modal "black boxes." The standard gradient methods of these CAD tools have turned out to be well appropriate for the optimizations. In Fig. 12(a), an iris compensated cross-junction is used for combining the filters. The overall scattering parameters of the optimized complete OMUX component are shown in Fig. 12(b). A manifold design is presented in Fig. 12(c). Fig. 12(d) shows the overall scattering parameters of the optimized complete OMUX component. The whole optimization of an

OMUX with the goal of 20-dB overall return loss at the common port typically took an overnight run on a hp715/100 workstation.

IV. Conclusion

Efficient mode-matching and hybrid mode-matching/numerical EM waveguide building blocks are described for the optimization-oriented use in powerful circuit CAD tools and the automated design of waveguide components. The building blocks allow the accurate and fast design of a very comprehensive class of rectangular and/or circular waveguide components including structures of more general shape. The designed waveguide structures are well appropriate for cost-efficient fabrication techniques, as no additional post-assembly tuning elements are required. The exciting advantages of using the waveguide building blocks in CAD tools include: fast and reliable customer-oriented waveguide designs are possible by utilizing powerful full-wave optimizers, accurate waveguide building blocks are conveniently available and full benefit can be taken of the design and graphical interface capabilities of matured CAD software.

Acknowledgment

The authors greatly acknowledge the kind suport of this challenging project by hp-EEsof, Westlake Village, CA, and by Optimization Systems Associates, Inc., Dundas, Ont., Canada, which placed their powerful CAD tools TOUCHSTONE and OSA90/hope, respectively, to the authors' disposal for the implementation of the mode-matching building block. The authors also wish to thank Mr. Hirsekorn, hp-EEsof, and Prof. Bandler, OSA, for their valuable help and stimulating discussions, Dr. Solbach, DASA, Ulm, Germany, and Dr. Hauth, Bosch Telecom, Backnang, Germany, for the fruitful cooperation and the many useful hints concerning optimized bend structures and the design of ridged waveguide filters, respectively.

References

[1] U. Papziner and F. Arndt, "Field theoretical computer-aided design of rectangular and circular iris coupled rectangular or circular waveguide cavity filters," *IEEE Trans. Microwave Theory Tech.,* vol. 41, pp. 462–471, Mar. 1993.

[2] Th. Sieverding and F. Arndt, "Field theoretic CAD of open or aperture matched T-junction coupled rectangular waveguide structures," *IEEE Trans. Microwave Theory Tech.,* vol. 40, pp. 353–362, Feb. 1992.

[3] W. Hauth, R. Keller, U. Papziner, R. Ihmels, T. Sieverding, and F. Arndt, "Rigorous CAD of multiport coupled rectangular waveguide components," in *Proc. 23rd European Microwave Conf.,* Madrid, Spain, Sept. 1993, pp. 611–614.

[4] Th. Sieverding and F. Arndt, "Rigorous analysis of the rectangular waveguide six-port cross junction," *IEEE Microwave Guided Wave Lett.,* vol. 3, pp. 224–226, July 1993.

[5] R. Keller and F. Arndt, "Rigorous modal analysis of the asymmetric rectangular iris in circular waveguides," *IEEE Microwave Guided Wave Lett.,* vol. 3, pp. 185–187, June 1993.

[6] P. Krauss and F. Arndt, "Rigorous mode-matching method for the modal analysis of the T-junction circular to sidecoupled rectangular waveguide," in *MTT-S Int. Microwave Symp. Dig.,* Orlando, FL, May 1995, pp. 1355–1358.

[7] T. Sieverding, J. Bornemann, and F. Arndt, "Rigorous design of sidewall aperture couplers," in *MTT-S Int. Microwave Symp. Dig.,* June 1993, vol. 2, pp. 761–764.

[8] U. Tucholke, F. Arndt, and T. Wriedt, "Field theory design of square waveguide iris polarizers," *IEEE Trans. Microwave Theory Tech.,* vol. MTT-34, pp. 156–160, Jan. 1986.

[9] J. Dittloff and F. Arndt, "Rigorous field theory design of millimeter-wave E-plane integrated circuit multiplexers," *IEEE Trans. Microwave Theory Tech.,* vol. 37, pp. 340–350, Feb. 1989.

[10] F. Arndt, U. Tucholke, and T. Wriedt, "Computer-optimized multisection transformers between rectangular waveguides of adjacent frequency bands," *IEEE Trans. Microwave Theory Tech.,* vol. MTT-32, pp. 1479–1484, Nov. 1984.

[11] F. Arndt, B. Koch, H.-J. Orlok, and N. Schroeder, "Field theory design of rectangular waveguide broad-wall metal-insert slot couplers for millimeter-wave applications," *IEEE Trans. Microwave Theory Tech.,* vol. MTT-33, pp. 95–104, Feb. 1985.

[12] J. Dittloff, F. Arndt, and D. Grauerholz, "Optimum design of waveguide E-plane stub-loaded phase shifters," *IEEE Trans. Microwave Theory Tech.,* vol. 36, pp. 583–587, Mar. 1988.

[13] F. Alessandri, G. Bartolucci, and R. Sorrentino, "Admittance matrix formulation of waveguide discontinuity problems: Computer-aided design of branch guide couplers," *IEEE Trans. Microwave Theory Tech.,* vol. 36, pp. 394–403, Feb. 1988.

[14] F. Allesandri, M. Mongiardo, and R. Sorrentino, "Computer-aided design of beam forming networks for modern satellite antennas," *IEEE Trans. Microwave Theory Tech.,* vol. 40, pp. 1117–1127, June 1992.

[15] F. Allesandri, M. Dionigi, R. Sorrentino, and M. Mongiardo, "A fullwave CAD tool of waveguide components using a high speed direct optimizer," in *IEEE MTT-S Int. Symp. Dig.,* San Diego, CA, May 1994, pp. 1539–1542.

[16] F. Allesandri, M. Dionigi, and R. Sorrentino, "A fullwave CAD tool of waveguide components using a high speed direct optimizer," *IEEE Trans. Microwave Theory Tech.,* vol. 43, pp. 2046–2052, Sept. 1995.

[17] J. M. Rebollar, J. Esteban, and J. Page, "Fullwave analysis of three and four-port rectangular waveguide junctions," *IEEE Trans. Microwave Theory Tech.,* vol. 42, pp. 256–263, Feb. 1994.

[18] J. Uher, J. Bornemann, and U. Rosenberg, *Waveguide Components for Antenna Feed Systems: Theory and CAD.* Norwood, MA: Artech House, 1993.

[19] A. A. Melecon, G. Connor, and M. Guglielmi, "New simple procedure for the computation of the multimode admittance or impedance matrix of planar waveguide junctions," *IEEE Trans. Microwave Theory Tech.,* vol. 44, pp. 413–418, Mar. 1996.

[20] O. P. Franza and W. C. Chew, "Recursive mode-matching method for multiple waveguide junction modeling," *IEEE Trans. Microwave Theory Tech.,* vol. 44, pp. 87–92, Jan. 1996.

[21] J. W. Bandler, R. M. Biernacki, S. H. Chen, R. H. Hemmers, and K. Madsen, "Electromagnetic optimization exploiting aggressive space mapping," *IEEE Trans. Microwave Theory Tech.,* vol. 43, pp. 2874–2882, Dec. 1995.

[22] Th. Sieverding, U. Papziner, T. Wolf, and F. Arndt, "New mode-matching building blocks for common circuit CAD programs," *Microwave J.,* vol. 36, pp. 66–79, Dec. 1993.

[23] ———, "Efficient design of rectangular and circular waveguide components using mode-matching simulators in common circuit CAD tools," in *Proc. IEEE MTT-S Int. Symp. Workshop,* Orlando, FL, May 1995.

[24] F. Arndt, Th. Sieverding, T. Wolf, and U. Papziner, "Optimization-oriented design of rectangular and circular waveguide components using efficient mode-matching simulators in commercial circuit CAD tools," *Int. J. Microwave MM-Wave Comp. Aided Eng.,* vol. 7, pp. 37–51, Jan. 1996.

[25] *Touchstone* or *Libra* by HpEEsof, Westlake Village, CA, USA.

[26] *Osa90/hope* by Optimization Systems Associates Inc., Dundas, Ont., Canada.

[27] J. F. Lee, "Analysis of passive microwave devices by using three-dimensional tangential vector finite elements," *Int. J. Num. Modeling,* vol. 3, pp. 235–246, Dec. 1990.

[28] P. P. Silvester and G. Pelosi, Eds., *Finite Elements for Wave Electromagnetics.* New York: IEEE Press, 1994.

[29] *Manual for High Frequency Structure Simulator.* Santa Rosa, CA: Hewlett Packard.

[30] A. Taflove, *Computational Electromagnetics: The Finite-Difference Time-Domain Method.* Norwood, MA: Artech House, 1995.

[31] J. Ritter and F. Arndt, "FD-TD/matrix pencil method for the efficient simulation of waveguide components including structures of more general shape," in *1996 MTT-S Int. Microwave Symp. Dig.,* June 1996, vol. 1, pp. 359–362.

[32] R. Beyer and F. Arndt, "Efficient modal analysis of waveguide filters including the orthogonal mode coupling elements by an MM/FE method," *IEEE Microwave Guided Wave Lett.,* vol. 5, pp. 1–3, Jan. 1995.

[33] J. R. Montejo-Garai and J. Zapata, "Full-wave design and realization of multicoupled dual-mode circular waveguide filters," *IEEE Trans. Microwave Theory Tech.*, vol. 43, pp. 1290–1297, June 1995.
[34] J. M. Reiter and F. Arndt, "Rigorous analysis of arbitrarily shaped H- and E-plane discontinuities in rectangular waveguides by a full-wave boundary contour mode-matching method," *IEEE Trans. Microwave Theory Tech.*, vol. 43, pp. 796–801, Apr. 1995.
[35] A. Weisshaar, M. Mongiardo, and V. K. Tripathi, "CAD-oriented equivalent circuit modeling of step discontinuities in rectangular waveguides," *IEEE Microwave Guided Wave Lett.*, vol. 6, pp. 171–173, Apr. 1996.
[36] A. Weisshaar, M. Mongiardo, A. Tripathi, and V. K. Tripathi, "CAD-oriented equivalent circuit models for rigorous full-wave analysis and design of waveguide components and circuits," in *IEEE MTT-S Int. Symp. Dig.*, San Francisco, CA, June 1996, pp. 1455–1458.
[37] H. Patzelt and F. Arndt, "Double-plane steps in rectangular waveguide and their application for transformers, irises, and filters," *IEEE Trans. Microwave Theory Tech.*, vol. MTT-30, pp. 771–777, May 1982.
[38] T. Sieverding and F. Arndt, "Modal analysis of the magic Tee," *IEEE Microwave Guided Wave Lett.*, vol. 3, pp. 150–152, May 1993.
[39] R. Beyer and F. Arndt, "Efficient modal analysis of waveguide filters including the orthogonal mode coupling elements by an MM/FE method," *IEEE Microwave Guided Wave Lett.*, vol. 5, pp. 9–11, Jan. 1995.
[40] Z. Shen and R. H. MacPhie, "An improved modal expansion method for two cascaded junctions and its application to waveguide filters," *IEEE Trans. Microwave Theory Tech.*, vol. 43, pp. 2719–2722, Dec. 1995.
[41] M. Guglielmi, G. Gheri, M. Calamia, and G. Pelosi, "Rigorous multimode network representation of inductive steps," *IEEE Trans. Microwave Theory Tech.*, vol. 42, pp. 317–326, Feb. 1994.
[42] J. J. H. Wang, *Generalized Moment Methods in Electromagnetics.* New York: Wiley, 1991.
[43] G. Conciauro, P. Arconi, M. Bressan, and L. Perregrini, "Wideband modeling of arbitrarily shaped H-plane waveguide components by the boundary integral-resonant mode expansion method," *IEEE Trans. Microwave Theory Tech.*, vol. 44, pp. 1057–1066, July 1996.
[44] W. Schroeder, and M. Guglielmi, "Boundary integral equation approach to multi-mode Y-matrix characterization of multi-ridged sections in circular waveguide," in *IEEE MTT-S Int. Symp. Dig.*, San Francisco, CA, June 1996, pp. 1849–1852.
[45] F. Giese, J. M. Reiter, and F. Arndt, "Modal analysis of arbitrarily shaped irises in waveguides by a hybrid contour-integral mode-matching method," in *IEEE MTT-S Int. Symp. Dig.*, Orlando, FL, May 1995, pp. 1359–1362.
[46] V. A. Labay and J. Bornemann, "Matrix singular value decomposition for pole-free solutions of homogeneous matrix equations as applied to numerical modeling methods," *IEEE Microwave Guided Wave Lett.*, vol. 2, pp. 49–51, Feb. 1992.
[47] O. C. Zienkiewicz, *The Finite Element Method.* Berkshire, U.K.: McGraw-Hill, 1977.
[48] J. Jin, *The Finite Element Method in Electromagnetics.* New York: Wiley, 1993.
[49] Y. Saad, "Numerical methods for large eigenvalue problems," in *Algorithms and Architectures for Advanced Scientific Computing.* Manchester, U.K.: Manchester Univ. Press, 1992.
[50] F. Arndt, T. Duschak, U. Papziner, and P. Rolappe, "Asymmetric iris coupled cavity filters with stopband poles," in *IEEE MTT-S Int. Symp. Dig.*, Dallas, TX, May 1990, pp. 215–218.
[51] M. Guglielmi, F. Montauti, L. Pellegrini, and P. Arcioni, "Implementing transmission zeros in inductive-window bandpass filters," *IEEE Trans. Microwave Theory Tech.*, vol. 43, pp. 1911–1915, Aug. 1995.
[52] G. Matthaei, L. Young, and E. M. T. Jones, *Microwave Filters, Impedance-Matching Networks, and Coupling Structures.* New York: McGraw-Hill, 1964.
[53] Y. Konishi and K. Uenakada, "The design of a band pass filter with inductive strip planar circuit mounted in waveguide," *IEEE Trans. Microwave Theory Tech.*, vol. MTT-22, pp. 869–873, Oct. 1974.
[54] F. Arndt, U. Papziner, Th. Sieverding, and T. Wolf, *WASP© operating Manual.* Bremen, Germany: Microwave Dept., Univ. of Bremen, Germany, 1994.
[55] Th. Sieverding and F. Arndt, "Combined circuit-field-theory CAD procedure for manifold multiplexers with circular cavities," in *Proc. 24th European Microwave Conf.*, Cannes, France, Sept. 1994, pp. 437–442.
[56] F. Arndt, J. Bornemann, D. Heckmann, C. Piontek, H. Semmerow, and H. Schueler, "Modal S-matrix method for the optimum design of inductively direct-coupled cavity filters," in *Proc. Inst. Elect. Eng.*, Oct. 1986, vol. 133, pt. H, pp. 341–350.
[57] H. Schmiedel, "Anwendung der Evolutionsoptimierung bei Mikrowellenschaltungen," *Frequenz*, vol. 85, pp. 306–310, 1981.
[58] J. Bornemann, R. Vahldieck, F. Arndt, and D. Grauerholz, "Optimized low-insertion-loss millimeter-wave fin-line and metal insert filters," *Radio Elec. Engineer*, vol. 52, pp. 513–521, Nov./Dec. 1982.
[59] J. W. Bandler, R. M. Biernacki, S. H. Chen, P. A. Grobelny, and R. H. Hemmers, "Space mapping technique for electromagnetic optimization," *IEEE Trans. Microwave Theory Tech.*, vol. 42, pp. 2536–2544, Dec. 1994.
[60] A. E. Williams, "A four-cavity elliptic waveguide filter," *IEEE Trans. Microwave Theory Tech.*, vol. MTT-20, pp. 258–265, Apr. 1972.
[61] J. D. Rhodes, "A low-pass prototype network for microwave linear phase," *IEEE Trans. Microwave Theory Tech.*, vol. MTT-18, pp. 290–302, June 1970.
[62] D. A. Bathker, "A stepped mode transducer using homogeneous waveguides," *IEEE Trans. Microwave Theory Tech.*, vol. MTT-15, pp. 128–129, Feb. 1967.
[63] K. Solbach, "Below-resonant-length slot radiators for traveling-wave-array-antennas," *Ant. Propag. Mag.*, vol. 38, no. 1, pp. 7–14, Feb. 1996.
[64] R. Beyer and F. Arndt, "Field-theory design of circular waveguide dual-mode filters by a combined mode matching finite element method," in *EuMC Int. Microwave Symp. Dig.*, Cannes, France, Sept. 1994, pp. 294–299.
[65] L. Accatino, G. Bertin, and M. Mongiardo, "A four-pole dual mode elliptic filter realized in circular cavity without screws," in *IEEE MTT-S Int. Symp. Dig.*, San Francisco, CA, June 1996, pp. 627–629.

Fritz Arndt (SM'83–F'93) received the Dipl.Ing. Dr.-Ing., and Habilitation degrees from the Technical University of Darmstadt, Darmstadt, Germany, in 1963, 1968, and 1972, respectively.

From 1963 to 1972, he worked on directional couplers and microstrip techniques at the Technical University of Darmstadt. Since 1972, he has been a Professor and Head of the Microwave Department, University of Bremen, Bremen, Germany. His research activities are in the area of the solution of field problems of waveguide, finline, and optical waveguide structures, antenna design, and scattering structures.

Dr. Arndt is a member of the VDE and NTG, Germany. He received the NTG Award in 1970, the A. F. Bulgin Award (together with three co-authors) from the Institution of Radio and Electronic Engineers in 1983, and the Best Paper Award of the Antenna Conference JINA 1986, France.

Ralf Beyer received the Dipl.-Ing. degree from the Technical University of Braunschweig, Germany, in 1992.

Since then he has been with the Microwave Department, University of Bremen, Bremen, Germany, where he is working on the Dr.-Ing. degree in electrical engineering. His research interests are currently related to the computer-aided design of waveguide components and antenna networks, based both on the finite-element and mode-matching method.

Jan Michael Reiter was born in Luebeck, Germany, in 1961. He received the Dipl.-Ing. degree from the University of Braunschweig, Germany, and the Dr.-Ing. degree from the University of Bremen, Bremen, Germany, both in electrical engineering, in 1989 and 1995, respectively.

Since 1990, he has been with the Microwave Department, University of Bremen, Germany. His research interests are currently related to the computer-aided design of passive waveguide components as well as on the modelling of cluster-feeds for shaped beam applications.

Thomas Sieverding (M'94) was born in Lohne, Oldenburg, Germany, in 1959. He received the Dipl.-Ing. and Dr.-Ing. degrees, both in electrical engineering, from the University of Bremen, Bremen, Germany, in 1984 and 1990, respectively.

From 1985 to 1987, he worked on software engineering at BICC Vero Electronics, Bremen. Since 1987, he has been with the Microwave Department, University of Bremen, and with OTCE-Consulting, Bremen. He has been an Assistant Professor at the University of Bremen since 1991. His research activities are focusing on computer-aided design techniques of satellite components and antenna networks.

Tomas Wolf was born in Bremen, Germany, on February 6, 1966. He received the Dipl.-Ing. degree in electrical engineering from the University of Bremen, Bremen, Germany, in 1993.

Since then he has been working for the Microwave Innovation Group (MIG), Bremen, developing software for microwave analysis and CAD programs.